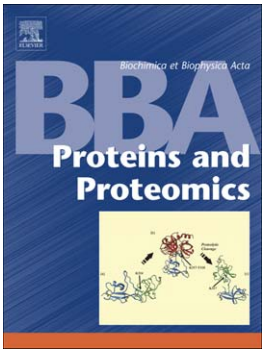

Structural and functional characterization of the phosphoglucomutase from *Xanthomonas citri* subsp. *citri*

Leandro Seiji Goto, André Vessoni Alexandrino, Camila Malvessi Pereira, Carla Silva Martins, Humberto D'Muniz Pereira, José Brandão-Neto, Maria Teresa Marques Novo-Mansur

PII: S1570-9639(16)30170-4
DOI: doi: 10.1016/j.bbapap.2016.08.014
Reference: BBAPAP 39805

To appear in: *BBA - Proteins and Proteomics*

Received date: 25 May 2016
Revised date: 17 August 2016
Accepted date: 23 August 2016

Please cite this article as: Leandro Seiji Goto, André Vessoni Alexandrino, Camila Malvessi Pereira, Carla Silva Martins, Humberto D'Muniz Pereira, José Brandão-Neto, Maria Teresa Marques Novo-Mansur, Structural and functional characterization of the phosphoglucomutase from *Xanthomonas citri* subsp. *citri*, *BBA - Proteins and Proteomics* (2016), doi: 10.1016/j.bbapap.2016.08.014

Title: Structural and functional characterization of the phosphoglucomutase from *Xanthomonas citri subsp. citri*

Authors: Leandro Seiji Goto[*1], André Vessoni Alexandrino[1], Camila Malvessi Pereira[1], Carla Silva Martins[1], Humberto D'Muniz Pereira[2], José Brandão-Neto[3], Maria Teresa Marques Novo-Mansur[1]

Affiliations: [1]Laboratório de Bioquímica e Biologia Molecular Aplicada - LBBMA, Departamento de Genética e Evolução, Universidade Federal de São Carlos, São Carlos, SP, Brazil; [2]Laboratório de Biologia Estrutural, Grupo de Cristalografia, Instituto de Física de São Carlos, Universidade de São Paulo, São Carlos, SP, Brazil, [3]Diamond Light Source, Harwell Science and Inovation Campus, Didcot, UK

[*]**Correspondence to:** Leandro S. Goto - Laboratório de Bioquímica e Biologia Molecular Aplicada - LBBMA, Departamento de Genética e Evolução, Universidade Federal de São Carlos, São Carlos, SP; Rod. Washington Luiz, km 235, Monjolinho, ZIP code 13565-905, PO Box 676, SP, Brazil; Phone/Fax: +55 (16) 3351-8788; E-mail: seiji_l@hotmail.com

ABSTRACT

Citrus canker, caused by bacteria *Xanthomonas citri subsp. citri*, can affect all economically important varieties of citrus. Studying *Xanthomonas* genes related to the invasive capacity may improve the knowledge on how this works and ultimately use the information to avoid the disease. Some annotated genes from *Xanthomonas citri subsp. citri* published genome are addressed to an interesting class of genes named "pathogenicity, virulence and adaptation". One of them is *xanA*, which encodes a predicted phosphoglucomutase. Phosphoglucomutases are ubiquitous enzymes among the living kingdoms that play roles in carbohydrate metabolism, catalyzing the reversible conversion of 1- to 6-phosphoglucose. In *Xanthomonas*, phosphoglucomutase activity is required to synthesize precursors of the pathogenesis-related polysaccharide xanthan. In this work, a characterization of this gene product is presented by structural and functional studies. Molecular cloning was used for heterologous expression and deletion of *xanA*. A Michaelis-Menten kinetics model was obtained using the recombinant protein. The protein structure was also determined by X-ray diffraction on the recombinant enzyme substrate-free, bound to glucose-1,6-biphosphate and to glucose-1-phosphate. Deletion of *xanA* was done with a suicide plasmid construct and the obtained mutant was tested for pathogenic capacity. This study is the first describing the properties of the *Xanthomonas citri* subsp. *citri* phosphoglucomutase.

KEYWORDS

Citrus canker; Xanthomonas *citri*; phosphoglucomutase; protein structure and function; gene deletion

Abbreviations: ASU, asymmetric unit; MPD, Methyl-2,4-pentanediol; PGM, Phosphoglucomutase.

1 - INTRODUCTION

Citrus canker caused by *Xanthomonas citri* subsp. *citri* is one of the most devastating diseases on citrus crops. It affects all commercial varieties and can easily spread on citrus growing areas worldwide. The disease causes local brownish corky lesions in all aerial parts of the plant, including leaf and fruit. Infected fruit loses quality due to lesions and productivity due to general premature fruit fall. Pathogen transmission is done by contact, either by natural agents like winds, rain, insects, or by human handling. As a major concern, there is no effective treatment nor prevention to the disease and the workaround is usually done by eradicating affected plants and groves [1].

Efforts made to better understand the mechanisms of infection include genomic [2-4], transcriptomic [5] and proteomic [6-8] studies as ways to indicate possible key molecules or mechanisms which could be used to control the disease. Random [9-11] and targeted [12-14] mutations are among the approaches commonly used on gene-to-disease correlation studies and the annotated genome [2] may provide initial perspectives on the selection of target genes. *X. citri* subsp. *citri* genomic records [2] describe a "pathogenicity, virulence and adaptation" gene class, which includes the gene *xanA* (XAC3579) encoding a predicted phosphoglucomutase (PGM). Our recent proteomics studies showed that *X. citri* subsp. *citri* PGM have positive differential expression from plain LB medium to pathogenicity-inducing medium (XAM-M), possibly indicating some involvement with the disease (Artier *et al.*, personal communication).

Phosphoglucomutases belong to the α-D-phosphohexomutase enzyme superfamily, widespread in all organisms. All enzymes in this superfamily catalyze the reversible conversion of 1- and 6-phosphosugars differing in the specific hexose [15] although some

PGMs may have bifunctionality, acting on both glucose and mannose [16-17]. All of them share general structural and functional features including a highly conserved phosphoserine residue in the active site that participates in the phosphoryl transfer, requirement of a divalent metal ion for activity and the same reaction mechanism. In brief, a monophosphoryl sugar is transiently converted into a biphosphorylated intermediate that is dephosphorylated and released as a product [18]. Catalyzing the conversion of glucose-1-phosphate (G1P) to glucose-6-phosphate (G6P), PGMs are enzymes (EC 5.4.2.2) that play roles in carbohydrate metabolism. G6P may efficiently follow the Glycolytic or Pentose Phosphate pathways, differently from G1P, the reverse reaction product which generally is involved in the glycogen metabolism [19-20].

Beyond the possible functions in energetic resources mobilization, a notable function of PGM in *Xanthomonas* comes from its relationship with pathogenicity, due to involvement in the biosynthesis of xanthan, an important interface in pathogen-plant interaction [21-22]. Activity of the *X. citri* subsp. *citri* PGM should provide 1-phophosugars for some precursors of xanthan [23-24].

In this work, molecular cloning was used to characterize the *xanA* (XAC3579) product, the predicted *X. citri* subsp. *citri* PGM, by functional and structural studies on the recombinant protein (XcPGM) and by infection studies with the deleted mutant.

2 - MATERIALS AND METHODS

2.1 - General procedures - *Xanthomonas citri* subsp. *citri* 306 was stored at -80° C in 20% v/v glycerol stocks. Custom oligonucleotides were provided by IDT. Restriction enzymes, PCR reagents and cloning vectors were supplied by Fermentas. pNPTS138 was kindly supplied by Prof. Dr. Ferreira H. (UNESP, Rio Claro-SP, Brazil). Other reagents were of

analytical grade or higher. Molecular biology techniques used throughout this work were described [25], or are detailed as follows.

2.2 - Cloning and construction of expression and deletion systems - Isolation of DNA fragments of interest was done by PCR using *X. citri* subsp. *citri* 306 genomic DNA as template. For recombinant expression purposes, PGM encoding sequence was amplified using oligonucleotides designed to incorporate an *Nde*I restriction site (underlined) at the 5' end of the PCR product (5'CCTTCATATGCCCATGACGCTACCCGCCTTC) and an *Xho*I site at the 3' extremity (5'TAGTATACTCGAGTCAGCCGCGCAGCAGGTTAG), right after XAC3579 predicted stop codon. For gene deletion, two distinct 1 kb regions adjacent to the PGM encoding sequence were individually amplified. For the upstream region, *Hind*III and *Bam*HI restriction sites were adapted to the 5' (5'TATATAAGCTTTTCCGACTGCAGCCACACATCGACG) and 3' (5'GTACTAGGATCCATCCTGAAGTGGGGGACGCC) ends respectively. For the downstream region, *Bam*HI (5'TATATCTAGGATCCTTGACCCCTCTCCCACCCATAGAC) and *Nhe*I (5' CAATAGCTAGCACCACATCCTCAAGCCCCACC) sites. PCR was performed using a C1000 Touch (Biorad) thermal cycler programmed to execute a 97° C initial 7 min denaturing step, followed by 35 cycles of 94° C for 30 s, 60° C 30 s, 72° C 1.5 min, and a final elongation step of 10 min at 72° C. Each fragment was amplified using 100 ng of genomic DNA and 100 pMol of each oligonucleotide on defined pair combinations in 50 µl reactions. Amplification products were gel-purified, cloned into pJET 1.2 (Fermentas) and transformed into *E. coli* DH5α for propagation. All the plasmids inserts were completely confirmed by sequencing [26] in a 3130 Genetic Analyzer (Applyed Biosystems). DNA

encoding PGM was excised using *Nde*I and *Xho*I restriction enzymes and subcloned into pET28a (Novagen) respective sites. The constructed plasmid provides IPTG induced expression of XcPGM fused to an *N*-terminal His-tag. The 1 kb regions were excised from the cloning vectors using their respective adapted restriction sites (*Hind*III-*Bam*HI and *Bam*HI-*Nhe*I) and sequentially subcloned into pNPTS138 (Alley Dickon, unpublished results) respective sites. The constructed deletion vector carries a kan^R selection marker and also provides sucrose suicide selection [27].

2.3 - Recombinant expression and protein purification – The expression vector was transformed into *E. coli* BL21 (DE3) (Novagen) and expression was carried out in an orbital shaker at 250 rpm, 18° C in LB broth added of 30 μg/mL kanamycin for 16 h after 0.1 mM IPTG addition to culture in mid-log growing stage. Cells from 1 L culture were collected by centrifugation and resuspended in 50 mL of 25 mM Tris-HCl pH 8.0 100 mM NaCl. Cell lysis was done by ultrasound pulses under ice bath and insoluble cellular debris were removed by centrifugation. Lysate soluble extract was loaded onto a 5 mL Ni-NTA column (Novagen) pre-equilibrated with the same buffer. For IMAC purification, column with bound protein was washed with 50 mL of 2 mM imidazole on the same buffer and purified XcPGM was eluted in 5 column volumes of 200 mM imidazole on the same buffer. Imidazole was removed by dialysis against 25 mM Tris-HCl pH 8.0 100 mM NaCl and XcPGM was stored at -20° C. Aliquots from every XcPGM preparation were routinely reserved for SDS-PAGE analysis [28] (not shown). Protein for crystallization was concentrated by ultrafiltration (Centriprep, Millipore) in 12.5 mM Tris-HCl pH 8.0 50 mM NaCl. XAC3579 encodes a putative 450 amino acid residues protein with molecular mass

of 49.1396 kDa. Measurement of PGM concentration was done by absorbance at 280 nm using a calculated [29] extinction coefficient of 0.1% ($g.L^{-1}$) = 0.842.

2.4 - Enzyme activity assay - PGM activity was measured [30] using Phosphoglucomutase Activity Assay Kit ab155896 (Abcam). Samples were prepared according to manufacturer instructions, except for the amount of substrate G1P which was adjusted for kinetics assays. Briefly, the assay infers G6P production by a glucose-6-phosphate dehydrogenase coupled reduction of NAD^+. NADH then reacts with a probe that begins to absorb light at 450 nm. Absorbance is converted to NADH equivalents by a standard curve, corresponding to G6P amount. Measurements were done in an iMark (Biorad) microplate reader, using clear flat bottom 96 well microtiter plates, recording the absorbance at 450 nm every 7 s along 20 min at 25° C. Initial enzyme velocities were estimated as the maximum linear rates of absorbance increase at 450 nm, using 0.0041 mg/mL XcPGM samples in 100 µL reactions (0.0834 µM). Absorbance values were correlated to product equivalent amounts with the standard curve equation $Abs_{450\ nm}$ = 0.0052 + 0.0822 x [NADH] and initial velocities were determined as a function of substrate concentrations. Substrate was varied from 4 x 10^4 to 19.53 µM G1P replacing water volume with a serial dilution of G1P, to a total volume of 100 µL. PGM activity was also tested on cell lysates aliquots of 50 µL from wild type *X. citri* subsp. *citri* and the *xanA* deleted mutant (XacΔ3579), also adjusted to a final volume of 100 µL.

2.5 - Protein crystallization and structure determination – XcPGM was prepared as described (section 2.3) and concentrated to 11 mg/mL in 12.5 mM Tris-HCl pH 8.0, 50 mM NaCl. Crystallization attempts were done using a Honeybee 939 liquid handler (Genomic Solution) with several available crystallization screens, by the vapor diffusion method.

Suitable XcPGM substrate-free crystals were obtained in condition A8 of Morpheus kit (Molecular Dimensions), which consists of 12.5 % PEG 1000, 12.5 % PEG 3350, 12.5 % MPD, 30 mM $MgCl_2$, 30 mM $CaCl_2$ and 100 mM MOPS/HEPES pH 7.5. Crystals appeared after 3 days and took a week to reach their maximum size (around 0.3 mm in the longest dimension). The substrate-free crystal was cooled in liquid nitrogen and diffraction data was obtained up to 1.27 Å resolution on beamline I24 at Diamond Light Source in the UK. The Xia2 software [31] was used for data processing. XcPGM structure was solved by molecular replacement using Phaser [32] and the structure of phosphoglucomutase from *Pseudomonas aeruginosa* (PDB ID 2FKF) [33], which shares 34% sequence identity, as a search model. The resultant solution was submitted to Arp/wArp [34] for automatic model building and the structure was refined using both Phenix [35] and Coot [36].

XcPGM ligand-bound structures were obtained using crystals from condition A4 of Morpheus kit (12.5 % PEG 1000, 12.5 % PEG 3350, 12.5 % MPD, 30 mM $MgCl_2$, 30 mM $CaCl_2$, 100 mM MES/Imidazole pH 6.5), after a 24 hours soaking with 2 mM of G1P or G1,6P. Then, crystals were diffracted in a Rigaku MicroMax 007 HF with R-AXIS IV++ (Rigaku Co.), using copper radiation at Laboratório de Biologia Estrutural, IFSC-USP. These data were processed with XDS Package [37]. XcPGM ligand-bound structures were also solved by molecular replacement using Phaser and the previously refined XcPGM ligand-free structure. Ligand sugars were positioned with Coot and refinements were performed using Phenix [35-36]. The behavior of R and R_{free} were used as main criteria for validating the refinement and stereochemical quality of the models evaluated with Molprobity [38]. Statistics of data processing and refinement are shown in Table 1.

The coordinates and structure factors for PGM substrate-free, G1P bound and G1,6P bound structures are deposited in the PDB (PDB IDs: 5BMN, 5BMP, 5KL0, respectively).

2.6 - Gene deletion and studies with the mutant (XacΔ3579) - As described before (section 2.2), two 1 kb flanking regions of the *xanA* structural gene were subcloned *in tandem* into pNPTS138. One μg of this constructed vector was used to transform electrocompetent cells of wild type *X. citri* subsp. *citri* strain 306 using a 0.2 cm gap cuvette in a Gene Pulser Xcell (Biorad) and parameters were 2.5 kV pulse, 200 Ω resistance and 25 μF capacitance. Transformants were selected on LB agar added of kanamycin. To obtain plasmid-free double crossing-over deleted mutants from these, an isolated transformant was grown for 24 h at 30° C, 250 rpm in LB broth without antibiotics. After that, 0.2 μL of the culture were spread over LB agar added of 10 % sucrose. As the constructed vector carries *sacB* suicide mark, growing colonies must lack the plasmid and should comprise both unchanged cells and the expected deleted mutant. Screening was done by PCR using another pair of oligonucleotides specific for *X. citri* subsp. *citri* genomic DNA, flanking 50 bp before the 1 kb upstream region and 50 bp after the 1 kb downstream region. Thus, deleted mutants are expected to show a PCR product around 2 kb while wild type should be close to 3.4 kb (see supplementary material).

Mutant and wild type cells were cultivated for 48 h at 30° C and 250 rpm in LB broth for both artificial infection of *Citrus aurantifolia* leaves [9] and native PGM activity tests. Cells were collected by centrifugation, washed twice with sterile water and resuspended to $OD_{600\ nm}$ = 0.59. Detached *Citrus aurantifolia* leaves were separately inoculated by spreading 10 μL of these bacterial suspensions over homogeneously pin

punctured areas on the abaxial surfaces and placed inside sterile clear tubes with 3 mL of sterile water. Negative control was done with sterile water. The development of infections was followed visually for 15 days at 25° C (see supplementary material). The remaining bacterial suspensions were added to 1 mM Tris-HCl pH 8.0 4 mM NaCl and lysed with ultrasound pulses. The lysates supernatants were used on the PGM enzymatic assay described before. Additionally, general colony morphology was monitored on plain LB agar and pathogeny inducing XAM-M medium, a derivative from XAM-1 [39] proposed by Prof. Dr. Ferro from Faculdade de Ciências Agrárias e Veterinárias de Jaboticabal, Universidade Estadual Paulista, UNESP-Jaboticabal, São Paulo, Brazil (unpublished).

3 - RESULTS

3.1 - Enzyme activity

Heterologous expression provided around 25 mg of purified XcPGM from 1 L of LB medium. XcPGM activity was estimated using an NAD^+ reduction probe coupled to G6P oxidation. Using G1P as substrate, PGM produces G6P, which is oxidized by glucose-6-phosphate dehydrogenase into 6-Phosphogluconolactone using NAD^+ as electron acceptor. NAD^+ is reduced to NADH which reacts with a probe that begins to absorb light at 450 nm. Hence, absorbance corresponds to G6P production and initial XcPGM reaction rates are recorded varying the amount of substrate G1P. Data is presented as a substrate saturation curve fitted in the Michaelis-Menten model (Figure 1). XcPGM has apparent V_{max} of 4.04 μmol/min/mg of protein and a K_m of 0.65 mM using G1P as substrate.

3.2 - Protein structure

XcPGM crystallized in orthorhombic space group $P2_12_12_1$ with one molecule per ASU and the crystals diffracted at high resolution (1.27-1.85Å) (Table 1). The general

structure (Figure 2A) is very similar to other PGMs, a globular protein with the four phosphohexomutase alpha/beta/alpha typical domains.

When compared by superposition, the ligand-free structures of XcPGM and *P. aeruginosa* PGM (PDB ID 1K35) showed an RMSd of 1.95Å. Major differences were observed in domain IV, especially in the orientation of helices 16 and 18 (residues 400-411 and 454-469 respectively), and beta-sheets were more conserved. Other subtle difference is observed in the turn between helices 5 and 6 of domain II.

The three XcPGM structures described here are quite similar to each other (Figure 2B), with an RMSd of 0.45Å (G1,6P-bound structure compared with ligand-free) and 0.131Å (G1P-bound with G1,6P-bound). The protein bound with either G1P or G1,6P shows a small decrease in both *b* and *c* cell dimensions (Table 1) to accommodate a small rotation in the domain IV. The major difference between ligand-free and bound structures is observed in the conformation of the second and third strands of the domain IV and the β-turn comprised by them (431-450), which is in "opened" conformation in ligand-free structure and in "closed" conformation in either G1P and G1,6P bound structures (Figure 2B). Indeed, seven (G1P) or eight (G1,6P) hydrogen bonds are formed between the ligand and the residues 431-450 (not shown). These hydrogen bonds can be responsible for the conformational change of this region upon ligand interaction. The conformational change is more pronounced in the β-turn region comprised by residues 436-445 and the greatest change is made by the Cα of T440, which moves 6.5 Å upon G1,6P binding.

3.3 - Structural characterization of the active site

In the XcPGM active site, both ligands G1P and G1,6P were readily identified in the standard Fo-Fc electron density maps contoured at 3σ (Figure 3A and B). Both ligands

induced several structural changes that can be used to characterize the XcPGM active site. The beta-hairpin where a conserved phosphoserine 119 lies changes its conformation upon ligand binding and the side chains of residues R34 and K129 adopt different rotamers. R34 in the ligand-free structure anchors two water molecules which are displaced upon ligand binding. Also, R34 side chain interacts with the D32 side chain (D32 OD1 - R34 NE, D32 OD2 - R34 NE and D32 OD2 - R34 NH2) until a ligand molecule arrives. Then, R34 side chain changes conformation opening the active site. The presence of the ligand also induces a conformational change in the main chain of the region 323-326 (between the third strand of the β-sheet 4 and the helix 11, and also in the side chain of H325). In the ligand-free structure, the side chain of H325 interacts with Y348 (H325 ND1 - Y348 OH). In ligand-bound structures, the region 323-326 moves toward the ligands and interactions of the main chain of H325 and the ligand are observed (H325 N - O3 (G1,6P) 2.8Å, N325 N - O4 (G1P) 3.1Å). Simultaneously, the interaction between H325 side chain and Y348 is lost. Also, there are minor displacements of side chains of R302, S344 and H346 induced by ligand binding.

In G1P binding, 15 hydrogen bonds are formed (2 water-mediated) in the active site (Figure 4A). Binding of the G1,6P involves the formation of 21 hydrogen bonds with the active site surroundings, six of them via water molecules (Figure 4B). One of these water molecules (w200 in G1,6P structure) is absent in the G1P complex, due to the sugar positioning. However, this structured water could possibly interact with glucose 6-phosphate (G6P), although only in the predictions as we did not obtain the XcPGM-G6P complex.

3.4 - Studies with the mutant

Two types of colonies were observed after plasmidial suicide selection on sucrose 10 %: a normal looking variety and a smaller, clearer, less viscous type (Figure 5). PCR screening confirmed that they were indeed the wild type and the expected deleted mutant respectively. Deleted mutants (XacΔ3579) showed a PCR product close to 2 kb whereas unchanged cells included the PGM 1.4 encoding region, showing a 3.4 kb product. Also, western blotting analysis confirmed lack of PGM (not shown). Further corroborating *xanA* deletion, XacΔ3579 lysates did not show PGM activity, different from the wild type (Figure 6). As an additional data, our tests indicated that *X. citri* subsp. *citri* should have around 5 x 10^{-12} PGM U/cell in the growth conditions we had used.

XacΔ3579 took 3 days to develop visible colonies on agar LB and 16 days on pathogenicity-inducing agar XAM-M, contrasting with the wild type that takes 2 and 3 days respectively. This indicates that although not being essential, PGM should have an important role on *X. citri* subsp. *citri* growing in XAM-M pathogenicity-inducing environment [39]. This correlates well with our local studies which indicated that PGM is differentially expressed from one medium to the other (Artier *et al.*, personal communication). However, *in vivo* experiments can provide better suited environment for correlation of PGM activity with the canker disease. Thus, detached *Citrus aurantifolia* leaves were simultaneously infected with either the mutant or the wild type strains as a way to compare the signs of the disease (Figure 7). Canker symptoms seemed relatively less severe in the mutant infection and both strains began to show the disease simultaneously, by the 5th day. This indicates that PGM could have some role, although not so determinant, in *X. citri* subsp. *citri* pathology.

4 - DISCUSSION

Here, we report a characterization of the PGM from *X. citri* subsp. *citri*. The protein structure was solved, functional parameters determined, and its importance on citrus canker development explored.

As observed in other PGMs [15, 33], the XcPGM active site is located in a cleft between domains I and IV. In domain I, a conserved phosphoserine residue (SEP119) was found phosphorylated in the three structures. Also, all the structures had a bound Mg^{2+} ion [40]. As previously discussed [41], a striking functional structure named invariant phosphate binding site (IPBS) should be formed in most (if not all) PGMs when in "closed" conformation, like the XcPGM ligand-bound structures. IPBS involves a set of four conserved residues placed in a common loop of domain IV plus one residue from domain I (respectively R421, S423, N424, T425 and Y17 in *P. aeruginosa*) that get close enough to hydrogen-bond a phosphate group from the incoming ligand phosphosugar. Additionally, a sixth residue (K285) is proposed to be recruited on IPBS formation only around 6-phosphosugar ligand moieties. All these elements (R436, S438, N439, T440 and Y31; K129 is only found in G1,6P complex) are conserved in XcPGM structure. Also, our structural data taken together comply with the G1,6P intermediate 180° reorientation mechanism proposed for phosphohexomutases [18, 33, 40].

Enzyme activity was studied using G1P as substrate, but based on sequence similarities, XcPGM appears to be closer to a bifunctional phosphomannomutase/phosphoglucomutases (PMM/PGM; EC 5.4.2.8) rather than a strict PGM [15]. Kinetic parameters vary considerably among PGMs [42] to establish some narrow rule. As an immediate comparison, the PMM/PGM from *Pseudomonas aeruginosa* [33], the closest sequence homolog (34 % identity, 52 % similarity) with solved structure

(PDB 2FKF), has a K_M around 27 µM. PGMs K_M values range from 0.003 mM for *Toxoplasma gondii* [43] to 3.5 mM for *Giardia lamblia* [16] and XcPGM lies within this range, being closer to *Sphingomonas paucimobilis* PGM K_M of 0.33 mM [17]. Rather than triggering catabolic pathways, relatively high G1P K_M values are proposed to describe enzyme forms that favor the synthesis of extracellular polysaccharides [44] (like xanthan for instance), which might be the case.

Although not studied here, it is reasonable to think that the PGM deletion should affect xanthan synthesis, hence impact on the pathogenicity, due to PGMs key role in the pathway [23, 45]. XacΔ3579 mutant colony morphology and delayed growth in pathogenicity-inducing medium XAM-M are consistent with that. However, we found that PGM did not seem crucial on artificial infection of *Citrus aurantifolia* leaves. On the contrary, wild type and mutant infection signs were barely different, although the deletion had a very evident effect on bacterial growth *in vitro*. Indeed, XacΔ3579 seemed to cause somewhat milder canker symptoms but still retained its infectivity. Perhaps this apparent discrepancy is more related to how much the XAM-M medium or the detached leaves infection method cannot emulate the natural infection than the relevance of *xanA* in the disease. Maybe other infection models, closer to the natural process or that quantify better the canker infection, could be more suitable to evaluate the influence of PGM on the disease. Such possibilities might be explored in future works but for now it is reasonable to speculate that PGM itself is not vital to canker progression.

5 - CONCLUSION

XanA, which encodes a predicted phosphoglucomutase in *X. citri subsp. citri* is required to synthesize the pathogenesis-related polysaccharide xanthan. As expected,

XcPGM kinetics indicates a role in the synthesis of G1P for precursors of xanthan. High-resolution structures of XcPGM provide a detailed view of the enzyme's active site and indicates the residues involved in catalysis. The deleted mutant clearly suffered impact from the lack of PGM, but curiously remained able to infect detached citrus leaves. However, the latter results should be taken with limitations at least due to the artificial infection methodology. PGM does not seem to be mandatory to the development of citrus canker symptoms but the impaired xanthan synthesis should affect citrus canker in some way.

6 - FUNDING

This work was supported by "Coordenação de Aperfeiçoamento de Pessoal de Nível Superior", CAPES-PNPD Institucional 23038.006942/2011-31 and "Fundação de Amparo à Pesquisa do Estado de São Paulo", FAPESP Proc. 07/50910-2.

REFERENCES

[1] A. Das, Citrus canker-A review, Journal of Applied Horticulture, 5 (2003) 52-60.
[2] A.C. da Silva, J.A. Ferro, F.C. Reinach, C.S. Farah, L.R. Furlan, R.B. Quaggio, C.B. Monteiro-Vitorello, M.A. Van Sluys, N.F. Almeida, L.M. Alves, A.M. do Amaral, M.C. Bertolini, L.E. Camargo, G. Camarotte, F. Cannavan, J. Cardozo, F. Chambergo, L.P. Ciapina, R.M. Cicarelli, L.L. Coutinho, J.R. Cursino-Santos, H. El-Dorry, J.B. Faria, A.J. Ferreira, R.C. Ferreira, M.I. Ferro, E.F. Formighieri, M.C. Franco, C.C. Greggio, A. Gruber, A.M. Katsuyama, L.T. Kishi, R.P. Leite, E.G. Lemos, M.V. Lemos, E.C. Locali, M.A. Machado, A.M. Madeira, N.M. Martinez-Rossi, E.C. Martins, J. Meidanis, C.F. Menck, C.Y. Miyaki, D.H. Moon, L.M. Moreira, M.T. Novo, V.K. Okura, M.C. Oliveira, V.R. Oliveira, H.A. Pereira, A. Rossi, J.A. Sena, C. Silva, R.F. de Souza, L.A. Spinola, M.A. Takita, R.E. Tamura, E.C. Teixeira, R.I. Tezza, M. Trindade dos Santos, D. Truffi, S.M. Tsai, F.F. White, J.C. Setubal, J.P. Kitajima, Comparison of the genomes of two Xanthomonas pathogens with differing host specificities, Nature, 417 (2002) 459-463.
[3] L.M. Moreira, N.F. Almeida, Jr., N. Potnis, L.A. Digiampietri, S.S. Adi, J.C. Bortolossi, A.C. da Silva, A.M. da Silva, F.E. de Moraes, J.C. de Oliveira, R.F. de Souza, A.P. Facincani, A.L. Ferraz, M.I. Ferro, L.R. Furlan, D.F. Gimenez, J.B. Jones, E.W. Kitajima, M.L. Laia, R.P. Leite, Jr., M.Y. Nishiyama, J. Rodrigues Neto, L.A. Nociti, D.J. Norman, E.H. Ostroski, H.A. Pereira, Jr., B.J. Staskawicz, R.I. Tezza, J.A. Ferro, B.A. Vinatzer, J.C. Setubal, Novel insights into the genomic basis of citrus canker based on the genome sequences of two strains of Xanthomonas fuscans subsp. aurantifolii, BMC Genomics, 11 (2010) 238.
[4] L.M. Moreira, R.F. De Souza, L.A. Digiampietri, A.C.R. Da Silva, J.C. Setubal, Comparative Analyses of Xanthomonas and Xylella Complete Genomes, OMICS: A Journal of Integrative Biology, 9 (2005) 43-76.
[5] G. Astua-Monge, J. Freitas-Astua, G. Bacocina, J. Roncoletta, S.A. Carvalho, M.A. Machado, Expression profiling of virulence and pathogenicity genes of Xanthomonas axonopodis pv. citri, J Bacteriol, 187 (2005) 1201-1205.
[6] M.R. Soares, A.P. Facincani, R.M. Ferreira, L.M. Moreira, J.C. de Oliveira, J.A. Ferro, M.I. Ferro, R. Meneghini, F.C. Gozzo, Proteome of the phytopathogen Xanthomonas citri subsp. citri: a global expression profile, Proteome Sci, 8 (2010) 55.
[7] A. Mehta, Y.B. Rosato, Differentially expressed proteins in the interaction of Xanthomonas axonopodis pv. citri with leaf extract of the host plant, Proteomics, 1 (2001) 1111-1118.
[8] A. Facincani, L. Moreira, M. Soares, C. Ferreira, R. Ferreira, M.T. Ferro, J. Ferro, F. Gozzo, J.F. de Oliveira, Comparative proteomic analysis reveals that T3SS, Tfp, and xanthan gum are key factors in initial stages of Citrus sinensis infection by Xanthomonas citri subsp. citri, Functional & Integrative Genomics, 14 (2014) 205-217.
[9] Q. Yan, N. Wang, High-Throughput Screening and Analysis of Genes of Xanthomonas citri subsp. citri Involved in Citrus Canker Symptom Development, Molecular Plant-Microbe Interactions, 25 (2011) 69-84.
[10] W. Lian, K.P. Jayapal, S. Charaniya, S. Mehra, F. Glod, Y.S. Kyung, D.H. Sherman, W.S. Hu, Genome-wide transcriptome analysis reveals that a pleiotropic antibiotic regulator, AfsS, modulates nutritional stress response in Streptomyces coelicolor A3(2), BMC Genomics, 9 (2008) 56.
[11] M.L. Laia, L.M. Moreira, J. Dezajacomo, J.B. Brigati, C.B. Ferreira, M.I. Ferro, A.C. Silva, J.A. Ferro, J.C. Oliveira, New genes of Xanthomonas citri subsp. citri involved in pathogenesis and adaptation revealed by a transposon-based mutant library, BMC Microbiol, 9 (2009) 12.

[12] P.A. Cappelletti, R.F. Dos Santos, A.M. do Amaral, R.A. Homem, T. Dos Santos Souza, M.A. Machado, C.S. Farah, Structure-Function Analysis of the HrpB2-HrcU Interaction in the Xanthomonas citri Type III Secretion System, PLoS ONE, 6 (2011) e17614.
[13] F. Malamud, P.S. Torres, R. Roeschlin, L.A. Rigano, R. Enrique, H.R. Bonomi, A.P. Castagnaro, M.R. Marano, A.A. Vojnov, The Xanthomonas axonopodis pv. citri flagellum is required for mature biofilm and canker development, Microbiology, 157 (2011) 819-829.
[14] M.L. Tondo, S. Petrocelli, J. Ottado, E.G. Orellano, The monofunctional catalase KatE of Xanthomonas axonopodis pv. citri is required for full virulence in citrus plants, PLoS ONE, 5 (2010) e10803.
[15] G.S. Shackelford, C.A. Regni, L.J. Beamer, Evolutionary trace analysis of the α-D-phosphohexomutase superfamily, Protein Science, 13 (2004) 2130-2138.
[16] S. Mitra, J. Cui, P.W. Robbins, J. Samuelson, A deeply divergent phosphoglucomutase (PGM) of Giardia lamblia has both PGM and phosphomannomutase activities, Glycobiology, 20 (2010) 1233-1240.
[17] P.A. Videira, L.L. Cortes, A.M. Fialho, I. Sá-Correia, Identification of the pgmG Gene, Encoding a Bifunctional Protein with Phosphoglucomutase and Phosphomannomutase Activities, in the Gellan Gum-Producing Strain Sphingomonas paucimobilis ATCC 31461, Applied and Environmental Microbiology, 66 (2000) 2252-2258.
[18] R. Mehra-Chaudhary, J. Mick, L.J. Beamer, Crystal Structure of Bacillus anthracis Phosphoglucosamine Mutase, an Enzyme in the Peptidoglycan Biosynthetic Pathway, Journal of Bacteriology, 193 (2011) 4081-4087.
[19] A. Lehninger, D. Nelson, M. Cox, Lehninger Principles of Biochemistry, W. H. Freeman, Place Published, 2008.
[20] W.A. Wilson, P.J. Roach, M. Montero, E. Baroja-Fernández, F.J. Muñoz, G. Eydallin, A.M. Viale, J. Pozueta-Romero, Regulation of glycogen metabolism in yeast and bacteria, FEMS microbiology reviews, 34 (2010) 952-985.
[21] F. Katzen, D.U. Ferreiro, C.G. Oddo, M.V. Ielmini, A. Becker, A. Puhler, L. Ielpi, Xanthomonas campestris pv. campestris gum Mutants: Effects on Xanthan Biosynthesis and Plant Virulence, J. Bacteriol., 180 (1998) 1607-1617.
[22] F.L. Chou, H.C. Chou, Y.S. Lin, B.Y. Yang, N.T. Lin, S.F. Weng, Y.H. Tseng, The Xanthomonas campestris gumD gene required for synthesis of xanthan gum is involved in normal pigmentation and virulence in causing black rot, Biochem Biophys Res Commun, 233 (1997) 265-269.
[23] R. Köplin, W. Arnold, B. Hötte, R. Simon, G. Wang, A. Pühler, Genetics of xanthan production in Xanthomonas campestris: the xanA and xanB genes are involved in UDP-glucose and GDP-mannose biosynthesis, J. Bacteriol., 174 (1992) 191-199.
[24] C.-H. Hung, H.-C. Wu, Y.-H. Tseng, Mutation in the Xanthomonas campestris xanA Gene Required for Synthesis of Xanthan and Lipopolysaccharide Drastically Reduces the Efficiency of Bacteriophage [phi]L7 Adsorption, Biochemical and Biophysical Research Communications, 291 (2002) 338-343.
[25] F.M. Ausubel, Short protocols in molecular biology : a compendium of methods from Current protocols in molecular biology, 5th ed., Wiley, Place Published, 2002.
[26] F. Sanger, S. Nicklen, A.R. Coulson, DNA sequencing with chain-terminating inhibitors, Proc Natl Acad Sci U S A, 74 (1977) 5463-5467.
[27] C.R. Guzzo, R.K. Salinas, M.O. Andrade, C.S. Farah, PILZ Protein Structure and Interactions with PILB and the FIMX EAL Domain: Implications for Control of Type IV Pilus Biogenesis, Journal of Molecular Biology, 393 (2009) 848-866.

[28] U.K. Laemmli, Cleavage of structural proteins during the assembly of the head of bacteriophage T4, Nature, 227 (1970) 680-685.
[29] E. Gasteiger, C. Hoogland, A. Gattiker, S. Duvaud, M.R. Wilkins, R.D. Appel, A. Bairoch, Protein Identification and Analysis Tools on the ExPASy Server, in: J.M. Walker (Ed.) The Proteomics Protocols Handbook, Humana Press Inc, Place Published, 2005, pp. 571-607.
[30] J. King, Phosphoglucomutase, in: H.U. Bergmeyer (Ed.) Methods of Enzymatic Analysis (Second Edition), Academic Press, Place Published, 1974, pp. 798-801.
[31] G. Winter, xia2: an expert system for macromolecular crystallography data reduction, Journal of Applied Crystallography, 43 (2010) 186-190.
[32] A.J. McCoy, R.W. Grosse-Kunstleve, P.D. Adams, M.D. Winn, L.C. Storoni, R.J. Read, Phaser crystallographic software, Journal of Applied Crystallography, 40 (2007) 658-674.
[33] C. Regni, A.M. Schramm, L.J. Beamer, The Reaction of Phosphohexomutase from Pseudomonas aeruginosa: STRUCTURAL INSIGHTS INTO A SIMPLE PROCESSIVE ENZYME, Journal of Biological Chemistry, 281 (2006) 15564-15571.
[34] S.X. Cohen, M. Ben Jelloul, F. Long, A. Vagin, P. Knipscheer, J. Lebbink, T.K. Sixma, V.S. Lamzin, G.N. Murshudov, A. Perrakis, ARP/wARP and molecular replacement: the next generation, Acta Crystallographica Section D, 64 (2008) 49-60.
[35] T.C. Terwilliger, P.D. Adams, R.J. Read, A.J. McCoy, N.W. Moriarty, R.W. Grosse-Kunstleve, P.V. Afonine, P.H. Zwart, L.-W. Hung, Decision-making in structure solution using Bayesian estimates of map quality: the PHENIX AutoSol wizard, Acta Crystallographica Section D, 65 (2009) 582-601.
[36] P. Emsley, B. Lohkamp, W.G. Scott, K. Cowtan, Features and development of Coot, Acta Crystallographica Section D: Biological Crystallography, 66 (2010) 486-501.
[37] W. Kabsch, XDS, Acta Crystallographica Section D, 66 (2010) 125-132.
[38] I.W. Davis, L.W. Murray, J.S. Richardson, D.C. Richardson, MOLPROBITY: structure validation and all-atom contact analysis for nucleic acids and their complexes, Nucleic acids research, 32 (2004) W615-619.
[39] K. Wengelnik, C. Marie, M. Russel, U. Bonas, Expression and localization of HrpA1, a protein of Xanthomonas campestris pv. vesicatoria essential for pathogenicity and induction ofthe hypersensitive reaction, J Bacteriol, 178 (1996) 1061-1069.
[40] Y. Lee, M.T. Villar, A. Artigues, L.J. Beamer, Promotion of enzyme flexibility by dephosphorylation and coupling to the catalytic mechanism of a phosphohexomutase, J Biol Chem, 289 (2014) 4674-4682.
[41] C. Regni, L. Naught, P.A. Tipton, L.J. Beamer, Structural Basis of Diverse Substrate Recognition by the Enzyme PMM/PGM from P. aeruginosa, Structure, 12 (2004) 55-63.
[42] W.J. Ray Jr, E.J. Peck Jr, Phosphomutases, in: D.B. Paul (Ed.) The Enzymes, Academic Press, Place Published, 1972, pp. 407-477.
[43] M. Imada, S. Kawashima, M. Kanehisa, T. Takeuchi, T. Asai, Characterization of α-phosphoglucomutase isozymes from Toxoplasma gondii, Parasitology International, 59 (2010) 206-210.
[44] C. Kvam, E.S. Olsvik, J. McKinley-McKee, O. Saether, Studies on recombinant Acetobacter xylinum alpha-phosphoglucomutase, Biochemical Journal, 326 (1997) 197-203.
[45] A. Ramos, I.C. Boels, W.M. de Vos, H. Santos, Relationship between Glycolysis and Exopolysaccharide Biosynthesis in Lactococcus lactis, Applied and Environmental Microbiology, 67 (2001) 33-41.

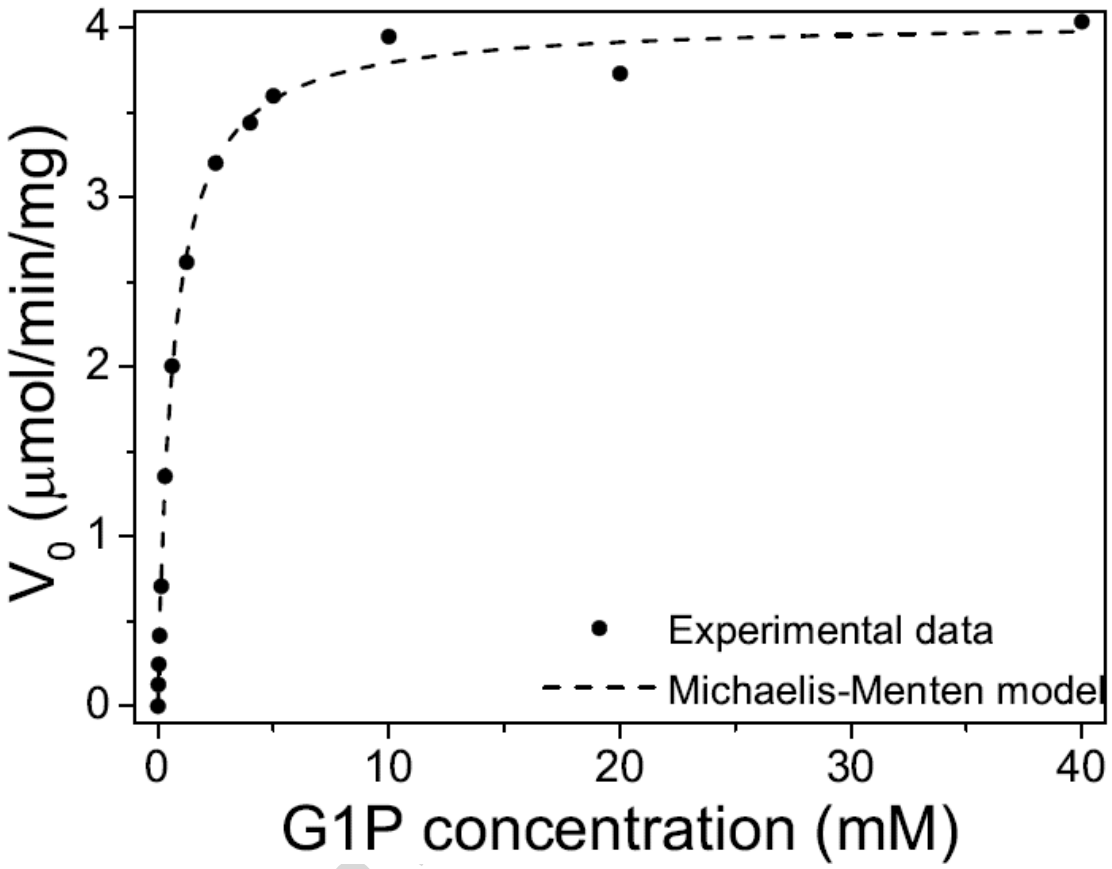

Figure 1

A

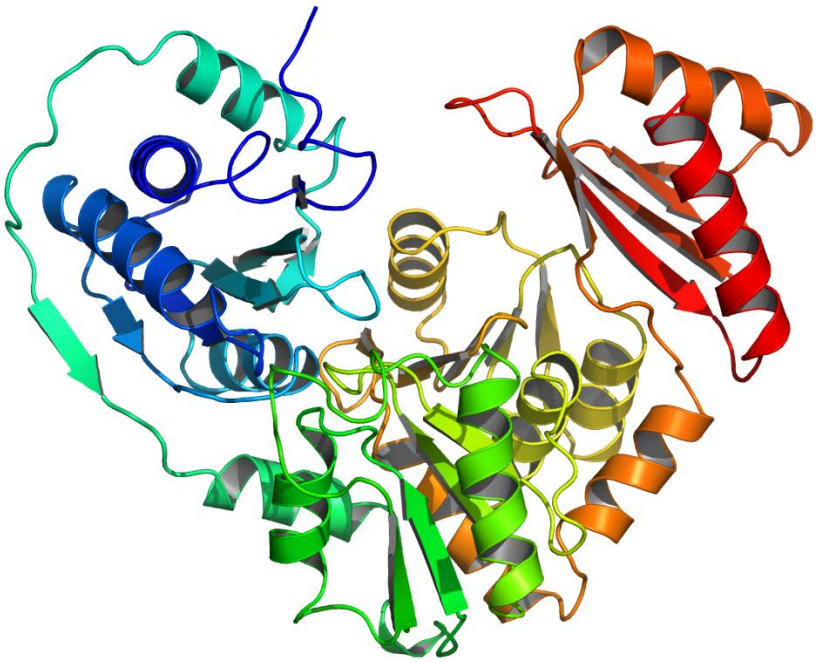

B

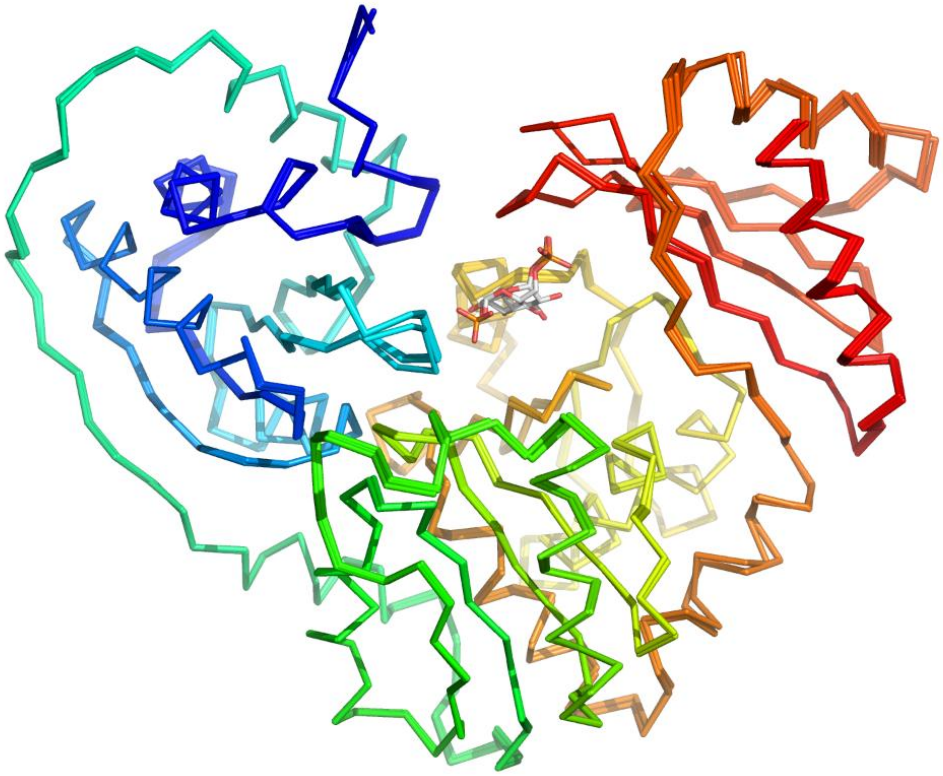

Figure 2

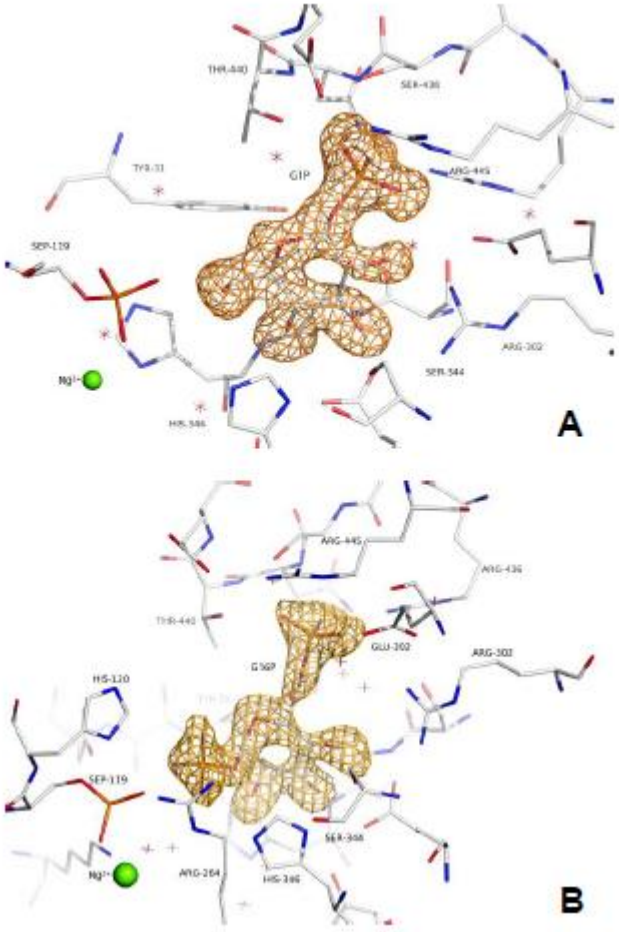

Figure 3

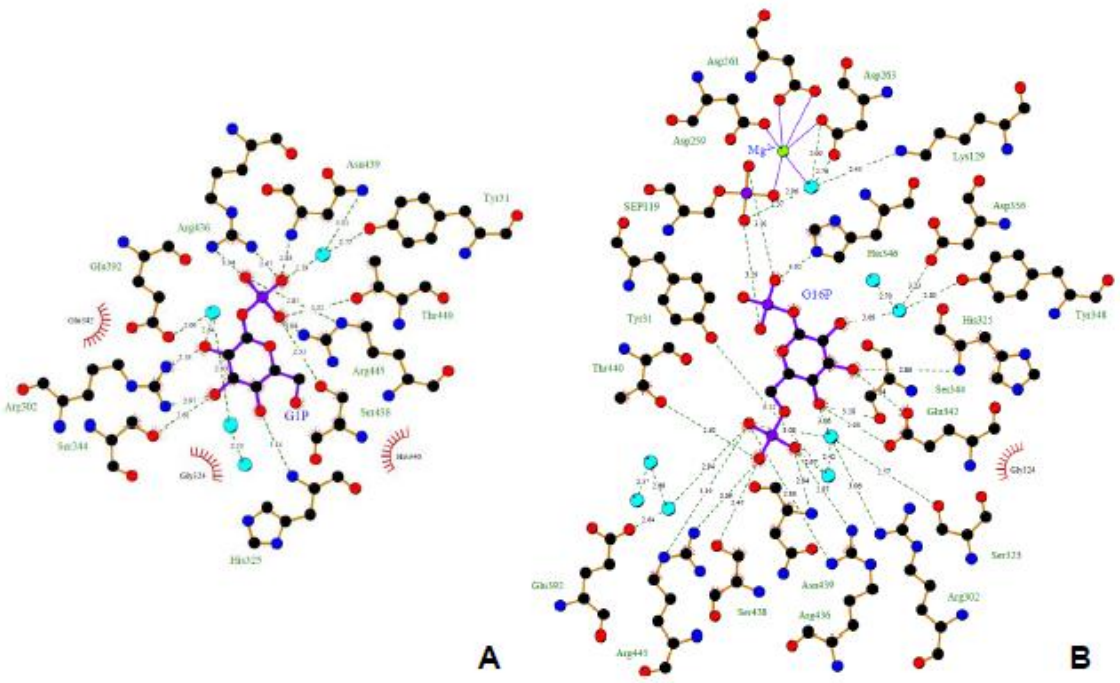

Figure 4

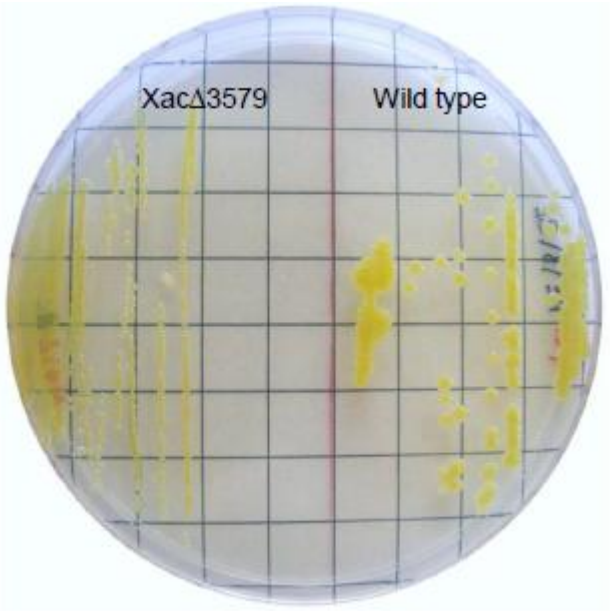

Figure 5

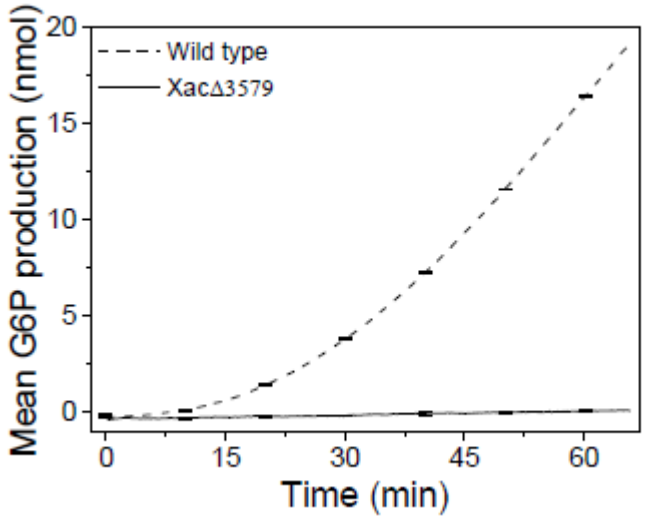

Figure 6

Figure 7

Table 1 - Statistics of XcPGM crystals data processing and refinement.

Data Collection	APO	G1P	G16P
Space Group	$P2_12_12_1$	$P2_12_12_1$	$P2_12_12_1$
Cell dimensions (Å) *a, b, c.*	43.98, 55.18, 174.70	43.90, 54.70, 173.20	43.98, 54.79, 173.50
Detector	PILATUS 6M	RIGAKU RAXIS IV$^+$	RIGAKU RAXIS IV$^+$
X-ray source	DLS I24	RIGAKU MicroMax 007 HF	RIGAKU MicroMax 007 HF
Wavelength (Å)	0.96861	1.541	1.541
Resolution range (Å)	52.62 - 1.27 (1.30 - 1.27)	20.00 - 1.85 (1.96 - 1.85)	20.00 - 1.85 (1.96 - 1.85)
Redundancy	6.3 (5.8)	3.13 (2.89)	3.71 (2.89)
*R*meas (%)*	4.5 (70.7)	2.3 (6.5)	2.4 (5.0)
CC (1/2)	0.999 (0.739)	1.00 (0.996)	1.00 (0.997)
Completeness(%)	99.6 (97.8)	98.4 (92.7)	97.4 (89.5)
Total reflections	713871 (46694)	135002 (15464)	132372 (14908)
Unique reflections	112663 (8100)	36040 (5343)	35635 (5146)
I / σ(I)	20.0 (2.8)	45.99 (17.74)	45.06 (22.89)
Refinement parameters			
Reflections used for	112557	36037	35633

refinement			
R (%)**	16.48	15.20	14.55
R_{Free}(%)**	18.69	17.97	18.51
No. of protein atoms	3450	3455	3450
No. of ligand atoms	0	17	21
B ($Å^2$)			
Protein	14.7	13.2	14.95
Ligand	---	21.80	31.13
Coordinate Error (ML based) (Å)	0.10	0.14	0.16
Phase error (^{o})	16.82	16.12	16.27
Ramachandran Plot			
Favored (%)	97.76	97.09	97.09
Allowed (%)	2.24	2.68	2.91
Outliers (%)	0.0	0.22	0.0
All-atom Clashscore	4.10	2.62	2.63
RMSD from ideal geometry			
r.m.s. bond lengths (Å)	0.007	0.004	0.008
r.m.s. bond angles (°)	1.118	0.866	0.893
PDB ID	5BMN	5BMP	5KL0

Highlights:

- *Xanthomonas citri* phosphoglucomutase structure was solved at high resolution;
- Structures were also obtained bound with substrates G1P and G1,6P;
- Phosphoglucomutase enzyme kinetics was studied using G1P as substrate;
- The *xanA* deleted mutant was obtained and caused milder canker symptoms.